Effect of burnt oil shale on ASR expansions: A petrographic study of concretes based on reactive aggregates

Alexandra Bourdot [a,b,*], Vincent Thiéry [a,b], David Bulteel [a,b], Jean-Gabriel Hammerschlag [c]

[a] Mines Douai, LGCgE MPE-GCE, F-59508 Douai, France
[b] University of Lille Nord de France, F-59000 Lille, France
[c] Holcim SA, MTS/PEM, CH-1312 Eclépens, Switzerland

HIGHLIGHTS

- Effect of burnt oil shale (BOS) on concretes based on reactive aggregate is studied.
- The expansion decreases from 17 wt% BOS with a flint aggregate.
- Expansions decrease with the BOS addition rate for siliceous limestone aggregates.
- Without BOS, ASR gel, microcracks and altered silica with alkalis are observed.
- The addition of BOS reduces the aggregate degradation and modifies gel products.

ARTICLE INFO

ABSTRACT

Some aggregates are potentially reactive and can be used because of a pessimum effect that allows reducing expansion. However some potentially reactive aggregates do not have this property and therefore cannot be employed. Thus, to valorise these potentially reactive aggregates, Supplementary Cementitious Materials (SCMs) can be added such as burnt oil shale which has been demonstrated to improve mechanical properties and inhibit ASR. This study proposed to employ burnt oil shale (BOS) from Germany and reports data on concrete based on a potentially reactive flint with a pessimum effect and two potentially reactive siliceous limestones. The action of burnt oil shale was observed in concrete expansions and aggregate degradation by SEM. At a microstructural scale, without burnt oil shale, aggregates are altered by ASR, i.e. the microcrystalline quartz for flint aggregate and finely dispersed microquartz for siliceous limestone aggregates present alkalis thanks to EDS analyses, which result in concrete expansion. The addition of burnt oil shale allows the reduction of aggregate degradation and modifies gel products with a lower C/S and a mix of C—S—H and ettringite for the flint concrete. Therefore, concrete expansion decreases approximately 90% from 17 wt% BOS with flint aggregate because of exploitation of the pessimum effect and with 30 wt% BOS for siliceous limestones. The burnt oil shale addition generates a competition between ASR and the pozzolanic reaction. The presence of micro-quartz in burnt oil shale would play a significant role in the pozzolanic reaction by fixing alkalis and thus inhibiting ASR.

© 2016 Elsevier Ltd. All rights reserved.

1. Introduction

The Alkali-Silica Reaction (ASR), defined for many years as one of the most damaging reactions in concrete, is defined by the reaction between concrete components: reactive aggregate, alkalis and portlandite from cement paste (more than 70% by moisture). Some aggregates such as flints [1–4] or siliceous limestones [5–11] are reactive. The ASR initiates the alteration of the crystal lattice and generates the aggregate reaction products responsible for concrete expansion. Moundoungou et al. demonstrated that the expansion depends on the capacity of reactive siliceous phases in aggregates to fix alkali ions thanks to EDS analyses by monitoring the increasing height of the alkali peaks [12]. Concrete expansion was observed when the neutralising capacity of the alkalis by the aggregate skeleton was exceeded, which generate aggregate degradation. The authors show that, for potentially reactive aggregates with the pessimum effect (PRP), it is possible to produce non

* Corresponding author at: GRESPI, University of Reims Champagne Ardenne, Moulin de la Housse, F-51687 Reims, France.
E-mail addresses: alexandrabourdot@gmail.com (A. Bourdot), vincent.thiery@mines-douai.fr (V. Thiéry), david.bulteel@mines-douai.fr (D. Bulteel), jean-gabriel.hammerschlag@holcim.com (J.-G. Hammerschlag).

expansive concrete. However, for potentially reactive aggregates (PR) such as, for example, some siliceous limestones, the issue of their use remains. To employ these potentially reactive materials, it is necessary to increase the capacity of the alkali neutralisation. Mineral additions are a way to reduce expansion due to ASR to valorise potentially reactive aggregates.

Various mineral additives have been used to limit the effects of ASR in concrete. Some additives were found to have a positive influence on the clinker substitution by accelerating hydration, but the positive influence depends on the alkalinity of the pore solution [13–15]. These additions are introduced into cement or added during the manufacture of the concrete. The additions may be of natural fine aggregates, burnt or raw materials such as finely milled burnt oil shale or industrial by-products such as blast furnace slag or fly ash. In the presence of mineral additions, the pozzolanic reaction could occur [16]. The process is complex and depends on the conditions and the proportion of pozzolan [17]. First, the reactive silica of pozzolans reacts with interstitial alkaline hydroxides [18]. Then, the calcium of CH from clinker hydration, combine with the silica and form pozzolanic C—S—H with a low calcium concentration [19] and varying proportions of water [20]. The pozzolanic C—S—H could fix alkalis [21]. Moreover, pozzolans are finely divided which gives them a dual benefit: a filler effect and a pozzolanic effect. Indeed, pozzolans allow further improvements of mechanical strength compared with fillers [22]. Thus, it would be more interesting to use pozzolan than fillers that are reactive in terms of decreasing ASR expansion. The use of mineral additions would be a way to fix alkalis to not exceed the threshold of alkali neutralization of the granular skeleton. A non-degraded concrete and therefore a valuation of potentially reactive aggregates would follow. Supplementary Cementitious Materials (SCMs) such as burnt oil shale [23] have been demonstrated to improve mechanical properties [24,25]. According to Winter [26], finely crushed burnt oil shale allow filling the voids as silica fumes and fly ashes. The employment of burnt oil shale to mitigate the ASR development in highly alkali cement seems to be available [27,28] and does not show manufacturing difficulties contrary to silica fumes that can generate in some cases, negative effects with the expansion of concrete [19,29]. Therefore, the burnt oil shale pozzolan will be added to the concrete studied in this paper.

Oil shales are present in the world as more than 600 deposits that represent approximately 11.5 trillion tons according to data from the 27th International Geological Congress [30] but numerous deposits are still largely unexplored. The European Academies Science Advisory Council (EASAC) summarises the European oil shale industry history [31]. The oil shale industry started in Scotland in 1696 to produce oil, hot water and finally electricity. The industrialisation of the oil shale exploitation began during the 19th century in Australia, the United States, Brazil, Germany and Scotland. During the 20th century, oil shale processing factories were built in several countries including China and Israel. Today, oil shales are exploited in Estonia, Russia, Brazil, Australia and Germany. The United States represent the most important resource in the world (70%) but the oil shale industry is currently the most developed in Estonia which represents only 17% of the resources in Europe and approximately 11 million tons of oil shale in 2000, whereas the world production of oil shale was of approximately 15 million tons in 2000 [32]. Indeed, oil shales are commonly extracted from a quarry and burnt at 500 °C to produce oil but also at 600–900 °C to produce energy. For example, in Estonia over 90% of the power is generated from oil shale. Nevertheless, the exploitation leads to residues such as burnt oil shale quantified as millions of tons each year. These burnt oil shales are often landfilled because of the hazardous waste classification. This production is predicted to grow because of the increasing costs of petroleum-based products, and oil shale presents opportunities

for supplying some of the fossil energy needs of the world in the years ahead. The World Energy Council has therefore reviewed energy resources such as oil shale [33]. However, the combustion temperature of 800 °C is also optimal to generate ash with a high pozzolanicity [34–36], particularly when the ash is finely crushed [23,35,37] such as burnt natural pozzolans [38–40]. Then, the ash can be used in the manufacture of cement as well as inhibiting deleterious ASR [24,25,27,41,42]. Burnt oil shales have been employed since 1920 for cement manufacturing. Precursor countries are Germany, Russia and China. The first patent goes back to 1918, when 40 patents were filed on the use of burnt oil shale use in cement production [43]. Burnt oil shale has been used in the manufacture of cement for decades [44–49]. The central Dotternhausen remains an example of the use of burnt oil shale. Indeed, 350,000 tons of oil shale (i.e. 210,000 tons of burnt oil shale) can produce 650,000 tons of cement per year according to Riedhammer [50]. Crushed oil shale from the Dotternhausen Power Plant in Germany (burnt for calorific capacity due to organic components) has-been blended with Portland clinker since the 1940's [45,51]. The industrial process taking place in Dotternhausen is explained and schematised by Thiéry et al. [52]. However, the lacking of information on the alkali-reactivity of this specific burnt oil shale requires further study. Thus, our publication focuses on the effects of burnt oil shale (BOS) from Dotternhausen as SCM on expansions due to ASR for three different aggregate materials: a potentially reactive flint aggregate with a pessimum effect, as in other studies [27], and also two potentially reactive siliceous limestones without the pessimum effect. The degrees of deterioration of silica forms in aggregates were observed with electron microscopy to improve the understanding of the mechanism and are put in parallel with concrete expansion.

2. Materials

2.1. Aggregates

Three aggregates have been used in this study: a potentially alkali-reactive aggregate with a pessimum effect and two potentially reactive aggregates. Their bulk whole-rock main element oxide compositions are given in Table 1.

The potentially reactive aggregate with the pessimum effect is a flint from Conchil le Temple in France. The flint reactive aggregate is used as a reference in this study and is named aggregate C. This aggregate is very reactive and has been studied previously [12]. Aggregate C is extracted from a coastal formation of chert pebbles [53]. The 4/14 mm coarse aggregate noted "cC" is added to 0/4 mm fine innocuous limestone extracted from a massive rock, denoted "fN" for the concrete specimen.

Table 1
Bulk whole-rock main element oxide compositions of aggregate materials by XRF +LOI, in wt%.

Element	LoD[b]	Aggregate fractions						
		fN	cC	fT	cT	fS	cS	BOS
Na_2O	0.1	<LoD	0.9	<LoD	<LoD	<LoD	<LoD	0.4
K_2O	0.1	0.1	<LoD	0.4	0.4	2.2	1.7	3.7
MgO	0.1	1.1	<LoD	0.8	0.9	1.9	1.9	2.2
CaO	0.1	52.0	<LoD	46.0	46.9	36.3	40.0	24.5
Fe_2O_3	0.1	0.4	0.7	0.6	0.5	4.6	3.7	10.3
Al_2O_3	0.1	0.6	0.2	1.7	1.7	5.7	4.2	17.8
SiO_2	0.1	2.1	97.9	13.2	10.3	20.6	16.9	28.3
SO_3	0.1	0.1	0.6	0.6	0.4	0.5	0.3	8.6
LOI[a]	0.04	43.5	0.7	36.2	38.5	27.4	30.4	4.9
Sum total	–	99.9	100.8	99.5	99.6	99.2	99.1	100.7

[a] LOI: loss on ignition obtained by TGA analyses.
[b] LoD: limit of detection.

Table 2
Potentially reactive silica forms identified in aggregates and their modal content.

Silica forms	Potential reactivity	Aggregates					
		fN	cC	fT	cT	fS	cS
Sub-euhedral quartz	Low	–	–	Main	Main	Minor	Minor
Anhedral quartz	Low	–	–	Main	Main	Main	Main
Quartz with undulose extinction	High	Minor	–	Minor	Minor	Main	Main
Chalcedony	Very high	–	Main	Minor	Minor	–	–
Microcrystalline quartz	Very high	–	Main	Minor	Minor	Minor	Minor
Dispersed micro- to crypto-quartz	Very high	–	–	Main	Main	Main	Main
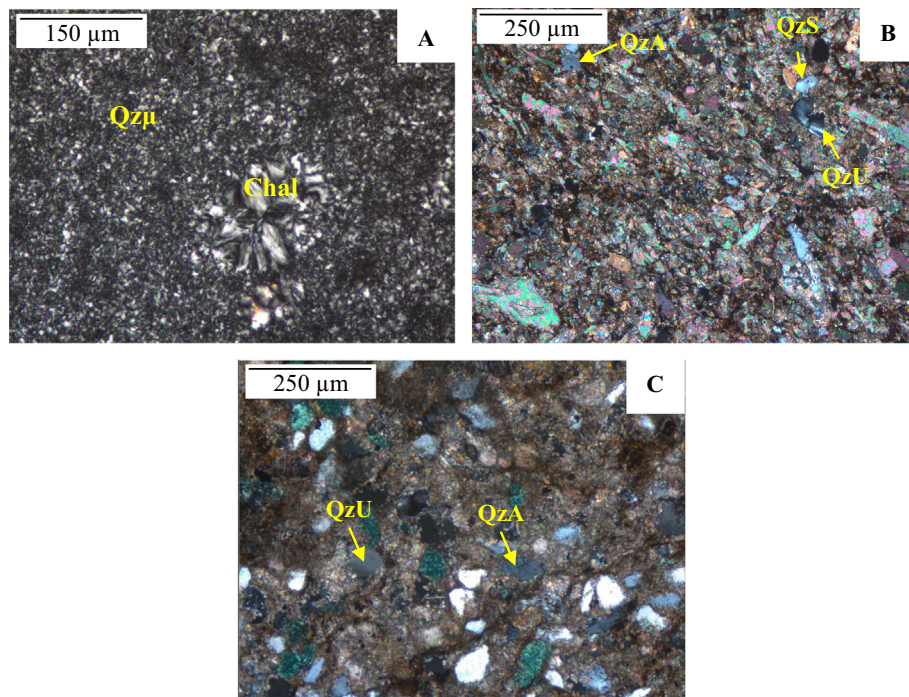
Fig. 1. Optical micrographs (transmitted light, uncrossed polar) of the flint aggregate C (A), siliceous limestone T (B) and S (C). Chal: chalcedony, Qzμ: microcrystalline quartz, QzA: anhedral quartz, QzS: Sub-euhedral quartz, QzU: Quartz with undulose extinction.

The two potentially reactive aggregates are siliceous limestones: the first comes from Belgium and the second comes from Switzerland. The Belgian siliceous limestone is extracted from a Tournai' quarry formed by different levels determined by the chemical composition of the material. The Belgian siliceous limestone has been recognized as potentially reactive [54,55]. The Belgian siliceous limestone used in this study is all derived from the mixture of different levels of the quarry. The 4/16 mm coarse aggregate and 0/4 mm fine aggregate are respectively noted "cT" and "fT". The Swiss siliceous limestone, named aggregate S is slightly metamorphic [56]. The sample comes from a specific area in the Albian strata of the quarry known as alkali-reactive, so the sample is not representative of all of the quarry. The sample presents a certain silica proportion that can induce responsiveness to ASR. The 4/16 mm coarse aggregate noted "cS" and the 0/4 mm fine aggregate noted "fS" are used. Silica types, their potential reactivity toward ASR and their relative proportions estimated by petrographic analysis in aggregates are listed in Table 2. The flint aggregate is essentially composed of microcrystalline quartz and chalcedony (Fig. 1A) and is therefore highly reactive. The two siliceous limestones are composed of some silica forms as sub-euhedral quartz, anhedral quartz and quartz with undulose extinction (Fig. 1B and C). Two very reactive forms are present in minor proportions: chalcedony and microcrystalline quartz (defined with a crystal size of less than 20 μm according to Flörke et al. [57]). Special attention is paid to the presence of the finely

dispersed micro- to crypto-quartz, respectively defined in the paper by a size of less than 10 μm [58] and 4 μm [59], as observed in other reactive aggregates [9,58,60] and highly reactive due to its size.

2.2. Supplementary Cementitious Material

Burnt oil shale used in this study is a residue from the combustion of so-called "Black Shales" from Dotternhausen Power Plant (Germany). Residues resulting from the calcination of oil shale are burnt oil shale (BOS). Burnt oil shale consists mainly of free lime, anhydrite, silica and calcite (Fig. 2). The other phases present in smaller proportions are iron oxides for example. Burnt oil shale is composed of nearly 10% sulphates (noted under SO_3 form) and 1.5% alkali in Na_2O_{eq}, mainly potassium. The composition of BOS presented in Table 1, has been considered to determine the percentage of clinker substitution by BOS in the manufacture of concrete mixtures. Indeed, BOS and gypsum bring some sulphates that can induce a delayed ettringite formation if too much gypsum (up to 7.5% as SO_3) were added to clinker, generating abnormal expansion.

The pozzolanicity of the BOS was determined. The procedure followed the NF EN 196-1 [61]. The blended mortars were prepared with 0 wt% (BOS0), 17 wt% (BOS1) and 30 wt% (BOS2) of the cement mass replaced by pozzolan. The specimens were tested for compressive strength at 1, 2, 7 and 28 days. The compressive
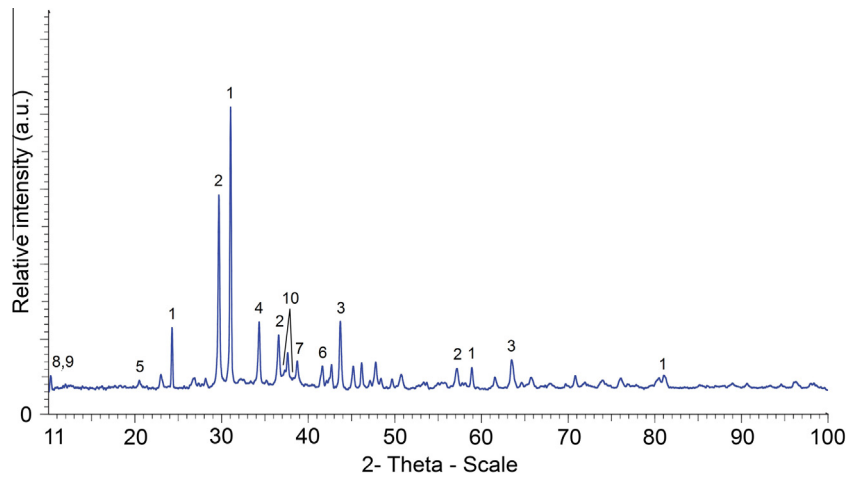
Fig. 2. XRD (Co-radiation) of burnt oil shale. 1: quartz, 2: anhydrite, 3: lime, 4: calcite, 5: dehydroxylated muscovite, 6: maghemite and magnetite, 7: hematite, 8: muscovite, 9: illite, 10: larnite (C_2S) and calcium aluminate (C_3A).

Table 3
Compressive strengths of mortars incorporating cement used in concrete specimens at 1, 2, 7 and 28 days and strength activity index at 7 and 28 days.

Mortars	BOS0	BOS1	BOS2
Compressive strength at 1 day (MPa)	15.3	15.3	17.1
Compressive strength at 2 days (MPa)	27.2	25.0	27.1
Compressive strength at 7 days (MPa)	42.8	42.3	45.0
Compressive strength at 28 days (MPa)	55.5	58.0	60.1
SAI at 7 days (%)	–	98.8	105.1
SAI at 28 days (%)	–	104.5	108.3

Table 4
Composition of the concrete mixtures tested.

Composition	Mixtures		
	cC+fN	cT+fT	cS+fS
Fine aggregate (34 vol%)	607	610	622
Coarse aggregate (66 vol%)	1215	1189	1200
Cement (kg/m^3)	410	410	410
Mix water (kg/m^3)	193	193	193
Bulk alkali content of concrete mixture (kg/m^3)	5.125	5.125	5.125
w/c	0.47	0.47	0.47
Bulk density (kg/m^3)	2425	2402	2424

Table 5
Main element oxide compositions of clinker and gypsum by XRF+LOI, in wt%.

Element	LoD[b]	Gypsum	Clinker
Na_2O	0.1	<LoD	0.5
K_2O	0.1	<LoD	0.5
MgO	0.1	0.1	1.0
CaO	0.1	32.7	65.5
Fe_2O_3	0.1	0.1	4.3
Al_2O_3	0.1	0.1	6.3
SiO_2	0.1	0.5	20.3
Mn_2O_3	0.1	<LoD	0.1
TiO_2	0.1	<LoD	0.4
P_2O_5	0.1	0.4	0.5
SrO	0.1	<LoD	0.2
SO_3	0.1	45.2	0.7
LOI[a]	0.04	20.7	0.1
Sum total		99.8	100.3

[a] LOI: loss on ignition obtained by TGA analyses.
[b] LoD: limit of detection.

3. Methods

3.1. Expansion tests

Concrete mixtures incorporating the aggregate materials mentioned above were prepared according to recommendations from Moundoungou et al. [10]. The alkali content of the bulk concrete was adjusted to 5.125 kg/m^3 through and initial proportion of 0.89% Na_2O_{eq} with the cement and the addition of NaOH to the mix water. The clinker is admixed with various amounts of burnt oil shale (0 wt% – BOS0, 17 wt% – BOS1, 30 wt% – BOS2). The ratios used are coarse on fine aggregate ratio of 2 and a water to cement ratio of 0.47. The proportions of concrete specimens are presented in Table 4. Concrete specimens were manufactured with clinker and gypsum from Obourg in proportions adapted to BOS addition. The clinker and gypsum compositions are in Table 5.

The binder used for reference concrete without BOS is equivalent to CEM I. Regarding the concrete with BOS, the clinker was substituted by 17 wt% and 30 wt% BOS to form an equivalent CEM II. Concrete specimens were tested for expansion at 38 °C. Indeed, according to Moundoungou et al. [10], testing at 60 °C in accordance with French standard NF P 18-454 and FD P 18-456 [65,66] generates mechanisms changing the observations by a reduction of the expansive behaviour versus temperature compared to testing at 38 °C. That change would be explained by a leaching of OH$^-$ out of the pore solution and a major diffusion

strengths are given in Table 3. Testing shows greater strengths for composed cements BOS1 and BOS2 compared to the control BOS0. The results are also expressed according to Eq. (1):

$$SAI = A/B \times 100. \tag{1}$$

where A is the unconfined compressive strength of the pozzolan mortar (MPa), and B is the unconfined compressive strength of the control mortar (MPa).

According to the NF EN 450-1 [62], a material is considered pozzolanic if SAI $\geqslant$ 75%. According to BS 3892 [63], SAI results greater than 80% after 28 days are indicative of a positive pozzolanic activity for fly ash for a cement replacement of 30 wt %. ASTM C618 [64] requires a SAI greater than 75% after 7 and 28 days for fly ash and natural pozzolans at a cement replacement of 20 wt%. Regarding BOS1 and BOS2 SAI (Table 3), they are greater than all of these specifications at 7 and 28 days; therefore, BOS is considered as pozzolanic material with respect to this method.

Table 6
Compressive strength of concrete specimens at 28 days, in MPa.

| Aggregates	BOS proportions		
	BOS0	BOS1	BOS2
cC+fN	56.6	58.0	65.3
cT+fT	53.7	56.0	60.5
cS+fS	49.3	58.4	60.1
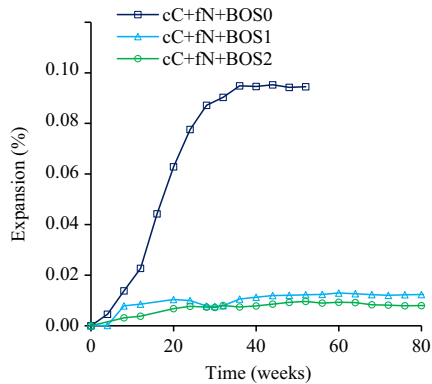
Fig. 3. Expansions of concrete based on flint aggregate without burnt oil shale (cC+fN+BOS0), 17 wt% (BOS1) and 30 wt% (BOS2) of burnt oil shale.

of alkalis with a more homogeneous repartition in aggregates. Consequently, experiments were performed using the French standard [65] but at 38 °C and 100%RH. The concrete specimens were prisms of dimensions 70 × 70 × 282 mm. The expansion test was performed on 6 prisms of the concrete mixtures.

Compressive strengths determinations of concrete specimens, performed on 150 × 150 × 150 mm cubes at 28 days, are presented in Table 6. The strength development is not affected by the use of BOS in the mixture. The BOS replacement has an impact on the mechanical properties of concrete specimens by an enhancement of compressive strengths by approximately 4–18% with 17 wt% BOS and 13–22% with 30 wt% BOS.
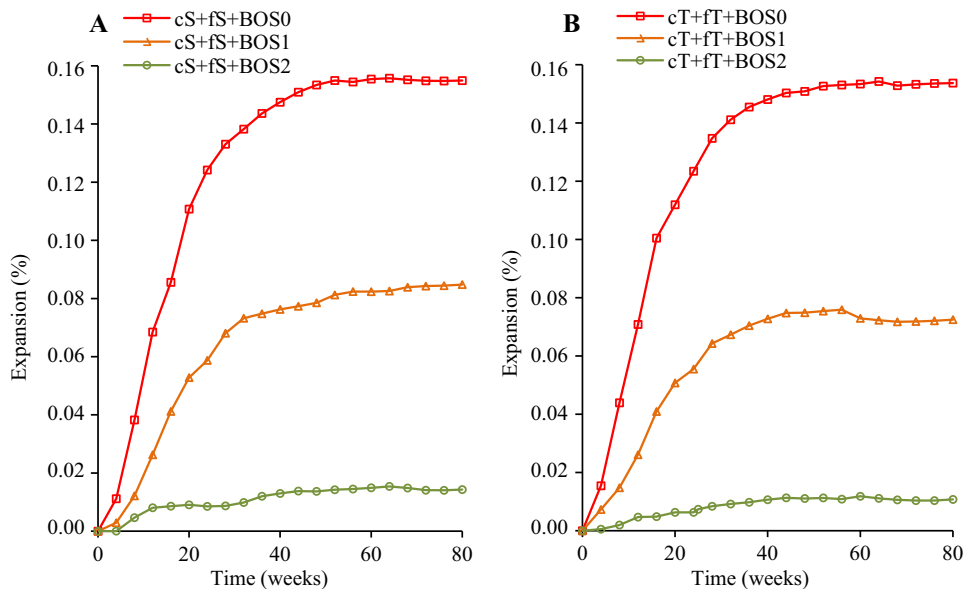
3.2. Petrography by SEM

The aim of this study was to describe microscopic deterioration, to link between characteristic ASR defects and expansion curves. Concrete specimens containing reactive aggregates (flint and siliceous limestone) and BOS, i.e., damaged concretes (BOS0) and undegraded concretes (BOS2) were studied. Concretes based on flint aggregate C, siliceous limestone T or S were studied by SEM at the beginning of the asymptotic expansion of curves at 38 °C. The petrography study was performed on polished sections from the concrete prisms. Between 3 and 5 thin sections were made for the concrete mixture selected. All of these samples were prepared and studied under the same conditions. The specimens were impregnated and hardened in a low-viscosity epoxy resin (Araldite 2020 from Huntsman) under vacuum at room temperature to prevent the material from breaking. Metal discs at 15 rotations per minute were used to remove saw marks. The samples underwent a sequential series of pre-polishing on SiC discs (Struers) with progressively finer grains (500; 1200; 2400; 4000 grit). Sections have been subsequently dry polished with diamond pastes (successive size of 6; 3; 1; 0.5; 0.25 μm) and subjected to ultrasonic cleaning with ethyl alcohol.

The petrographic study was carried out on concrete polished sections. An FEG-HITACHI S-4300SE/N Scanning Electron Microscope (SEM) equipped with a Thermoscientific Ultradry EDS (Energy Dispersive X-ray Spectroscopy) detector was employed to highlight cracks, ASR products, altered burnt oil shale and more or less degraded silica in the aggregates. To identify the presence of alkalis in siliceous phases, EDS semi-quantitative analyses were performed. Viewing and imaging techniques were equally employed using backscatter electron (BSE) and secondary electron (SE) imaging. SEM analyses were performed at an accelerating voltage of 20 kV, a working distance of 15 mm, between the probe and the sample, at a current of the order of 3 nA and a dead time of 20% on average in the EDS detector. The increase in the intensity of the alkali signals was considered to be proportional to their enrichment in part of the grains analyzed according to the principle given by [67]. The relative intensity of an X-ray line is approximately proportional to the mass concentration of the element investigated. All of the spots were recorded under the same conditions (one minute by spot) to allow comparison between them.

Fig. 4. Expansions of concrete based on siliceous Swiss limestone S (cS+fS) (A) and siliceous Tournai limestone T (cT+fT) (B) without burnt oil shale (BOS0) and with 17 wt% (BOS1) and 30 wt% (BOS2) of burnt oil shale.

4. Results

4.1. Longitudinal expansions of concrete specimens

Regarding the concrete based on Conchil the Temple flint aggregate, cC+fN, at 38 °C, the expansion is approximately 0.1%. By adding 17 wt% of burnt oil shale (cC+fN+BOS1), an expansion of 0.01% is shown in Fig. 3, which is confirmed when adding 30 wt% of BOS with a lower expansion. The pessimum effect of the reactive aggregate C was operated after 80 weeks, and the expansion was decreased from approximately 0.1% to 0.01% by the addition of a very small quantity of silica, brought by burnt oil shale.

In the case of the siliceous limestones T and S without BOS, concrete expansions exceeded 0.02% with approximately 0.16% at 38 °C, as shown in Fig. 4. The expansion was reduced by using burnt oil shale. A marked decrease in expansion is noticed between BOS concretes (BOS1 and BOS2) and ordinary concretes (BOS0). The decrease in expansion is proportional to the increasing rate of BOS addition. Expansion of the mix with BOS1 decreases by half to 0.08%. For the mix with BOS2, the expansion is low to only 0.01%, and so this mix does not present degradation.

Thus, it is necessary to use more burnt oil shale in siliceous limestone concrete than in flint concrete. As a result, used blended cements of BOS show themselves to be effective but the added BOS quantity depends on the reactive aggregate used.

4.2. Microstructural ASR effects

4.2.1. Concrete based on PRP flint "cC+fN"

Concretes based on aggregate C without burnt oil shale (CC+FN +BOS0) show a degradation related to ASR according to SEM observations. Indeed, the flint aggregates have characteristic cracks (Fig. 5A) previously observed by other authors in reactive aggregates [eg. 2,12,68,69]. Silica in the form of microcrystalline quartz in flint aggregate is altered and appears lumpy (Fig. 5B). The porosity is thus significantly increased. At the interface between the aggregates and the cement paste as well as cracks, expansive ASR reaction products are present with a C/S ratio of approximately 0.5 and contain alkalis Na and K (Fig. 5C). The degraded silica was analysed by SEM-EDS. Alkalis are present both at the interfacial zone (Fig. 5D) and in the particle of the aggregate (Fig. 5E). Their proportions are as important as the distance to the interface cement paste/aggregate decrease. The substitution of clinker by 30 wt% burnt oil shale (cC+fN+BOS2) avoids major degradation of the microcrystalline quartz. Aggregates exhibit no marked alteration and the surface has a dense microstructure (Fig. 6A). This silica in flint aggregates, affected little or not affected at all, presents little or no alkalis. SEM-EDS analyses have effectively demonstrated the presence of low sodium close to the interface with the cement paste (Fig. 6B). In the same way, no alkalis are detected in the aggregate (Fig. 6C). Reaction products can be observed
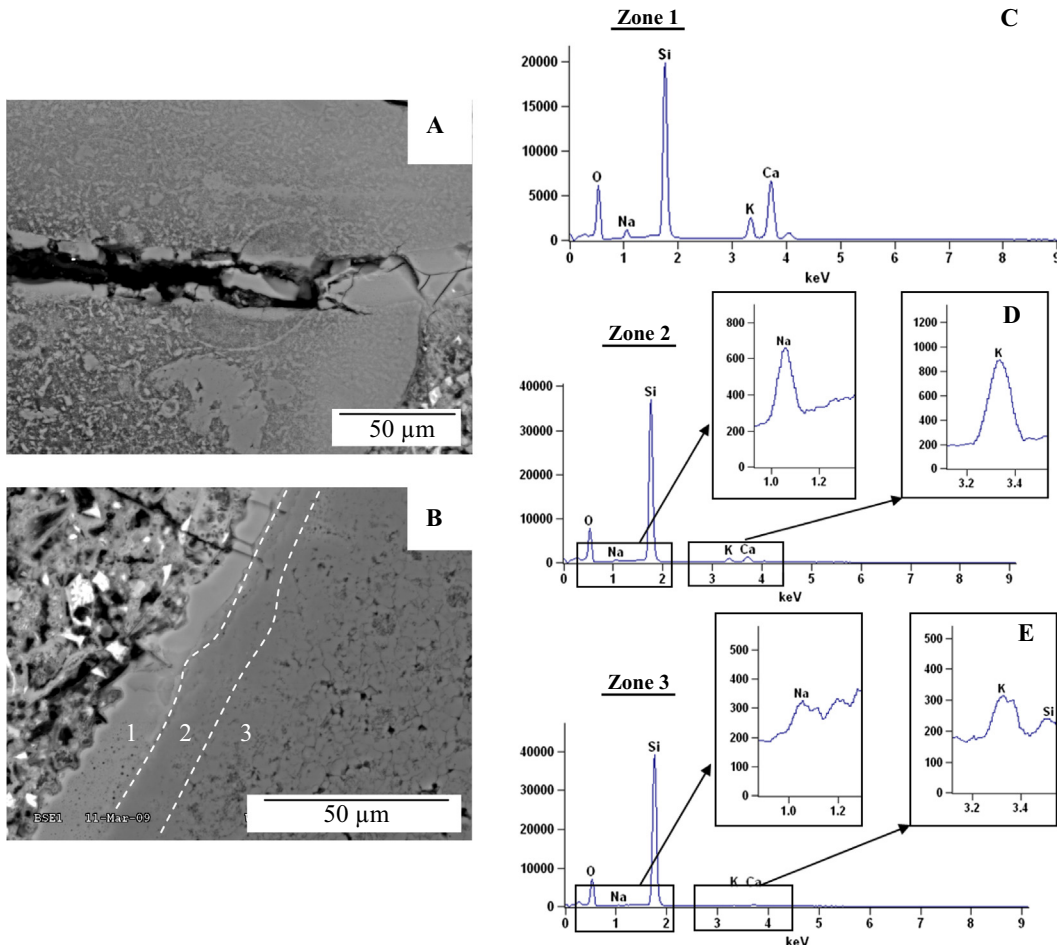

Fig. 5. ASR degradation in flint of concrete mixture "cC+fN+BOS0" observed by SEM: cracked flint and ASR gel (A), cement paste/aggregate interfacial zone (B). EDS spectrum of C—(K,N)—S—H in zone 1 (C), internal zone 2 (D) and altered flint with alkalis in zone 3 (E) from (B).
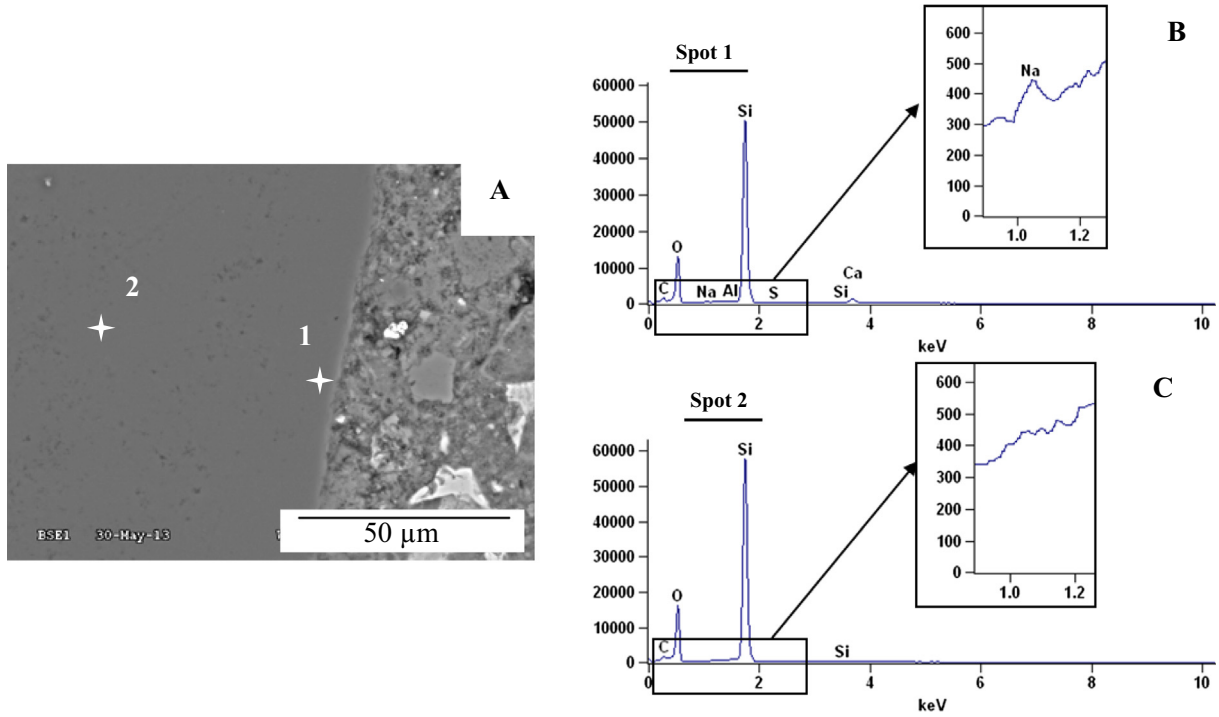
Fig. 6. Undegraded flint in concrete cC+fN+BOS2 (A). EDS spectrum of cement paste/aggregate interfacial zone with few alkalis (B) and in the aggregate without alkali (C).
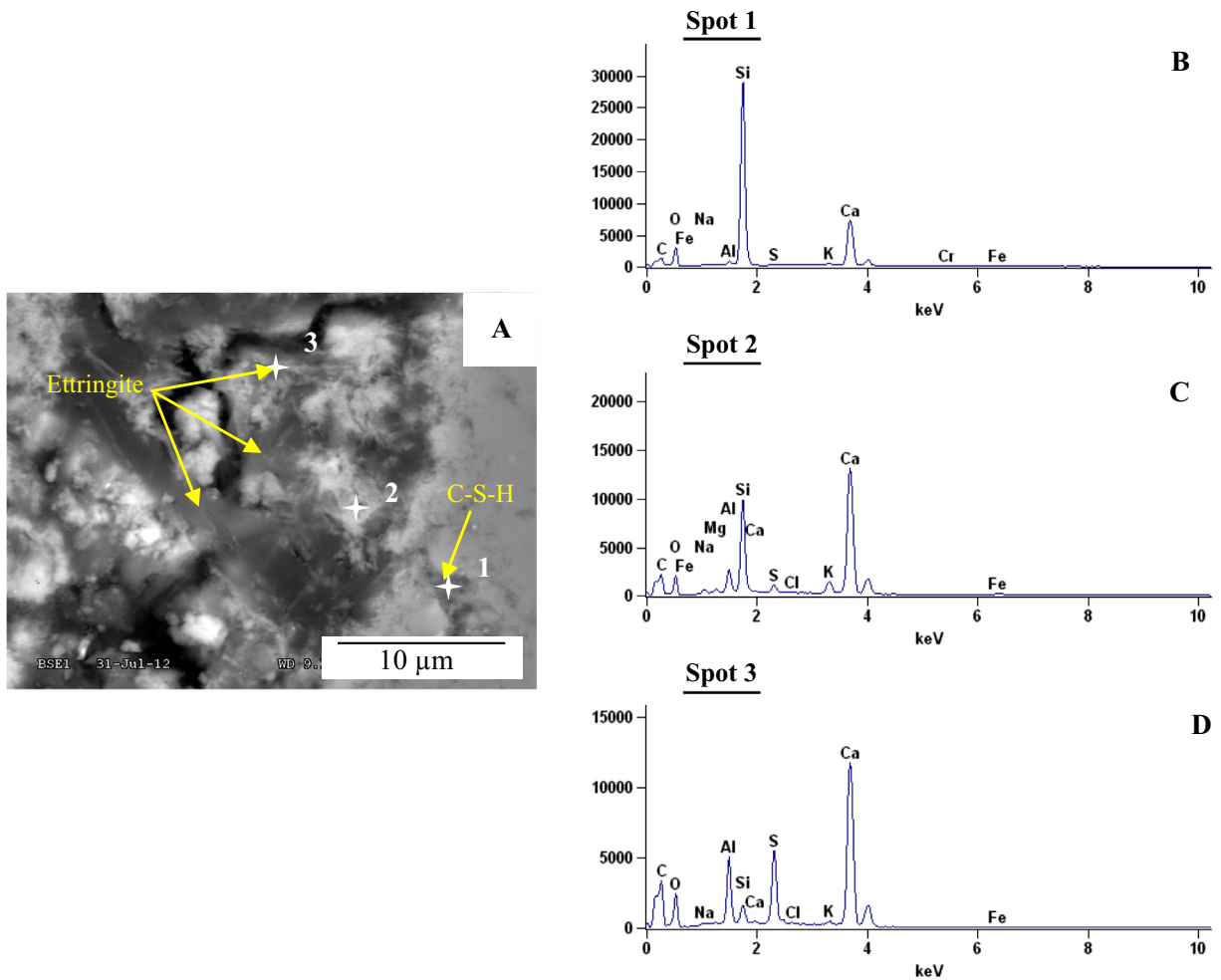

Fig. 7. Reaction products near an interface aggregate/cement paste in concrete cC+fN+BOS2 (A). EDS Spectrum of gel (B), a mixture of gel and ettringite (C), and ettringite (D).
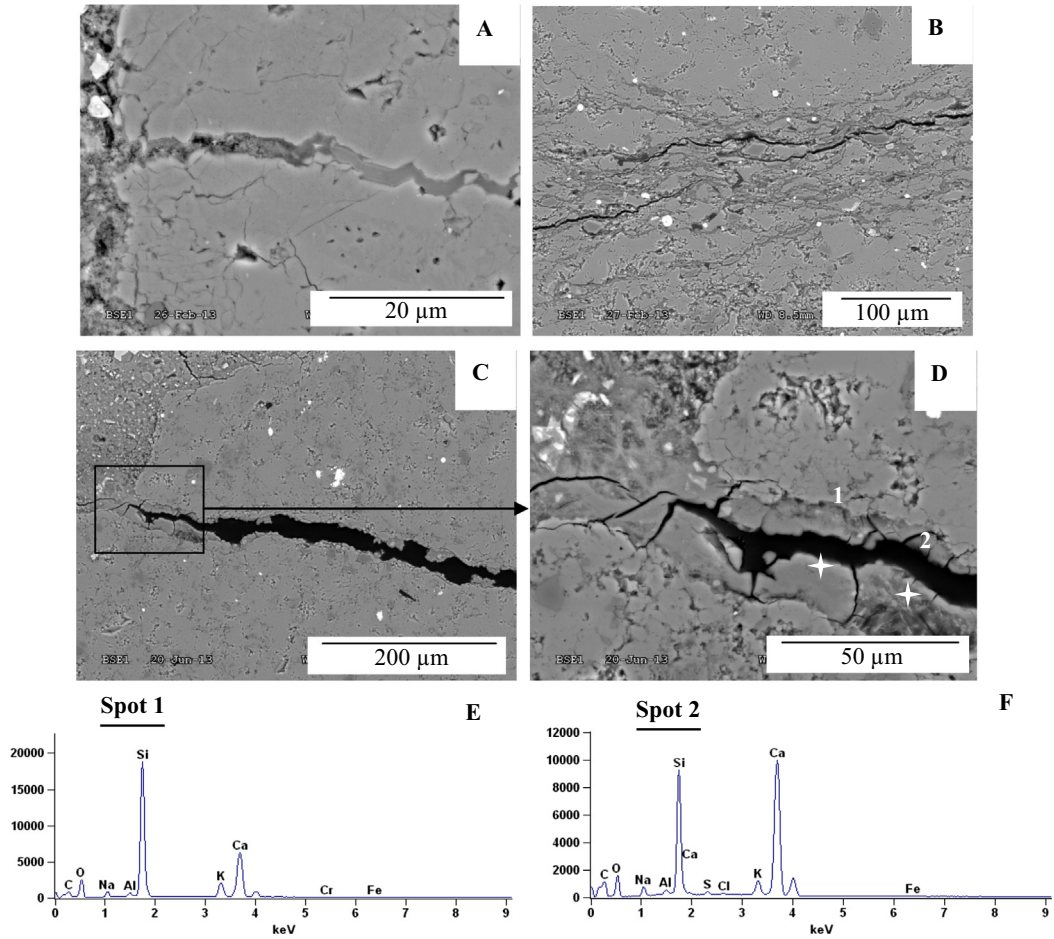
Fig. 8. ASR degradation in an aggregate of concrete mixture cT+fT+BOS0: cracks with ASR products (A), cracks as clay veins orientation (B), large crack in an aggregate (C) with ASR reaction products (D). EDS spectrum of ASR reaction products from (D), with variable C/S ratios (E and F).
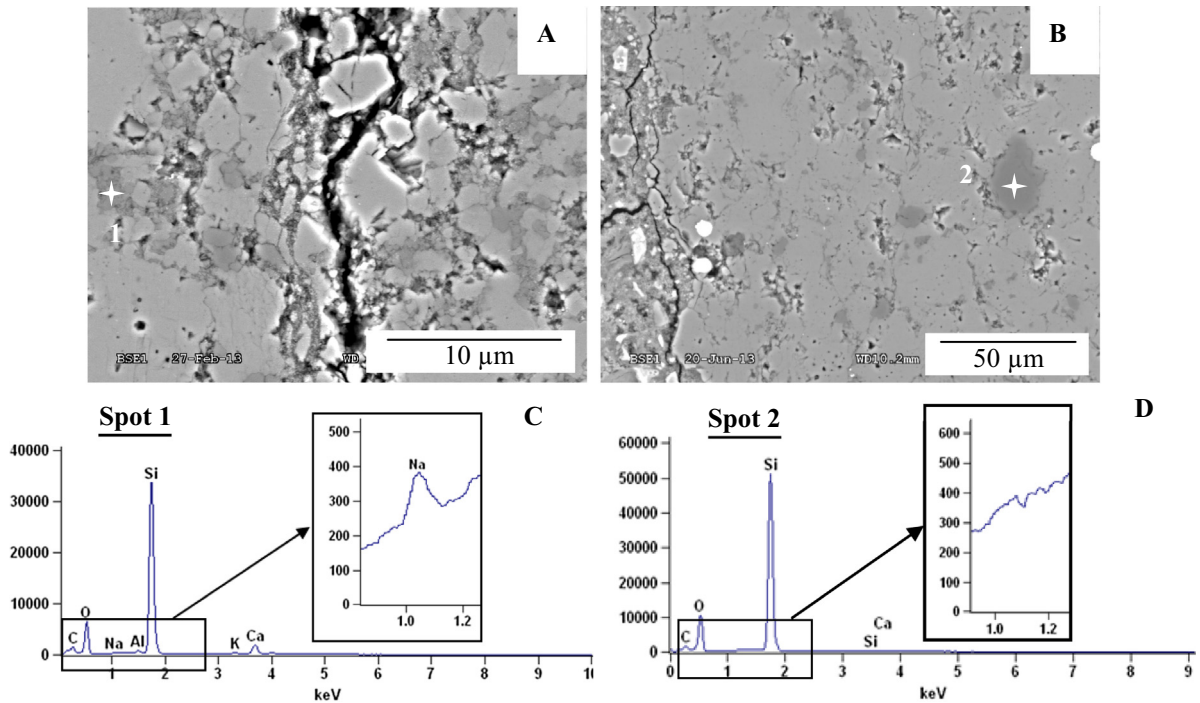
Fig. 9. Degraded siliceous limestone in concrete mixture cT+fT+BOS0: degraded micro-quartz <10 μm (A) and undegraded quartz >20 μm (B). EDS spectrum of micro-quartz with alkali Na (C) and large quartz without alkalis (D).
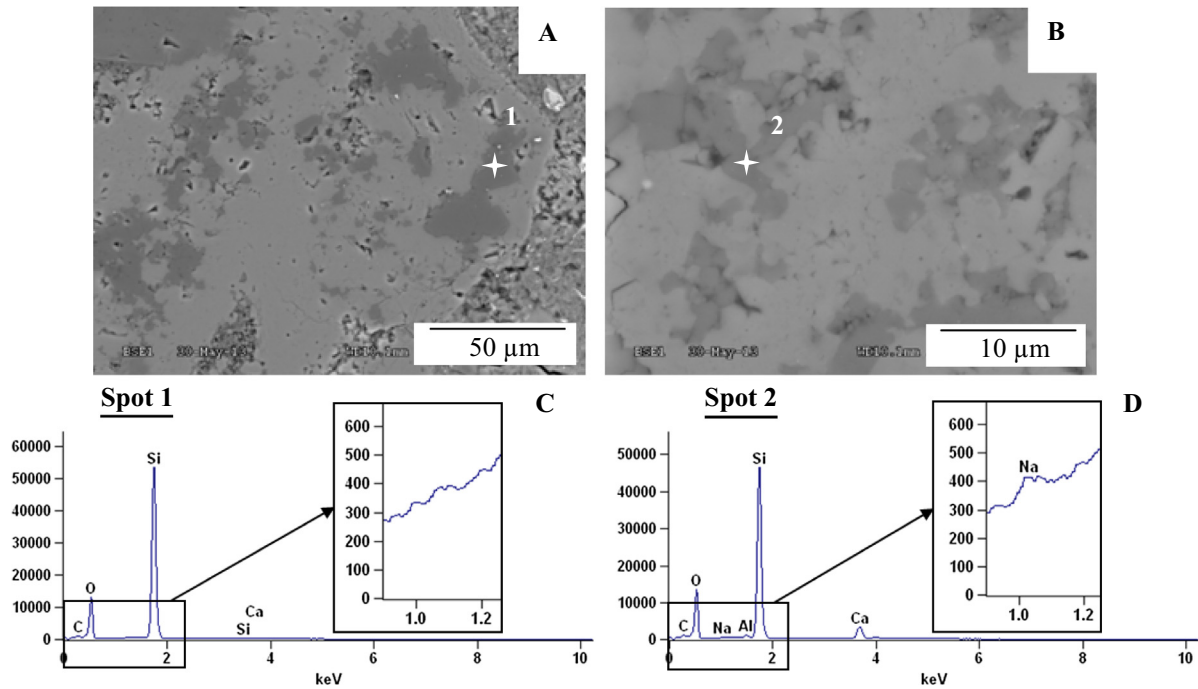
Fig. 10. Undegraded siliceous limestone in concrete mixture cT+fT+BOS2: undegraded quartz >20 μm (A) and micro-quartz <10 μm (B). EDS spectrum of large quartz without alkalis (C) and micro-quartz without alkalis (D).
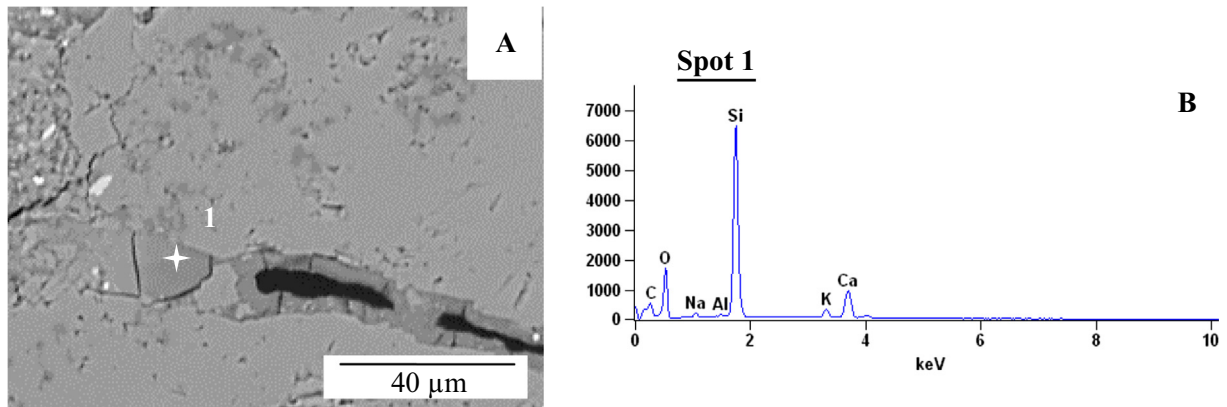
Fig. 11. Rare gels in siliceous limestone observed in concrete cT+fT+BOS2 (A). EDS spectrum of the C–S–H (B) from (A).
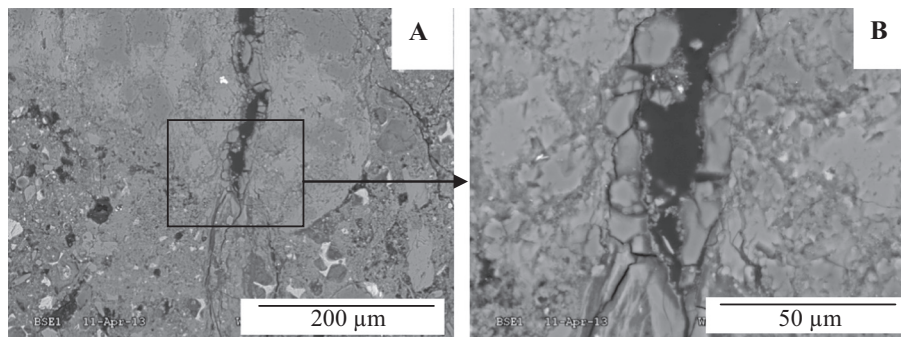

Fig. 12. ASR degradation in the aggregate of concrete mixture cS+fS+BOS0 observed by SEM (A): large crack at the interface aggregate/cement paste with ASR products (B).

(Fig. 7A) as a gel at the interface with the aggregate with a C/S ratio of approximately 0.4 and alkalis Na and K (Fig. 7B) and then as a gel mixture with ettringite moving away from the interface (Fig. 7C) to finish with only ettringite in the farthest area (Fig. 7D).

4.2.2. Concrete based on PR siliceous limestone
4.2.2.1. "cT+fT".

Concrete incorporating gravel and sand siliceous limestone T without burnt oil shale (cT+fT+BOS0) has large cracks (Fig. 8). These
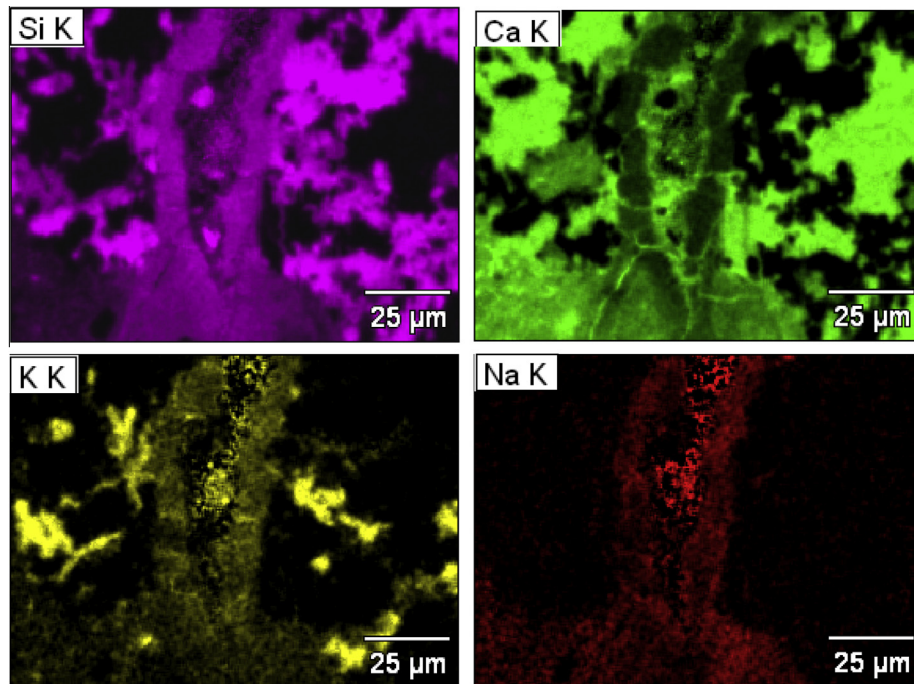
Fig. 13. Elemental X-ray images of altered concrete cS+fS+BOS0 from Fig. 12B: crack with C—(K,N)—S—H.
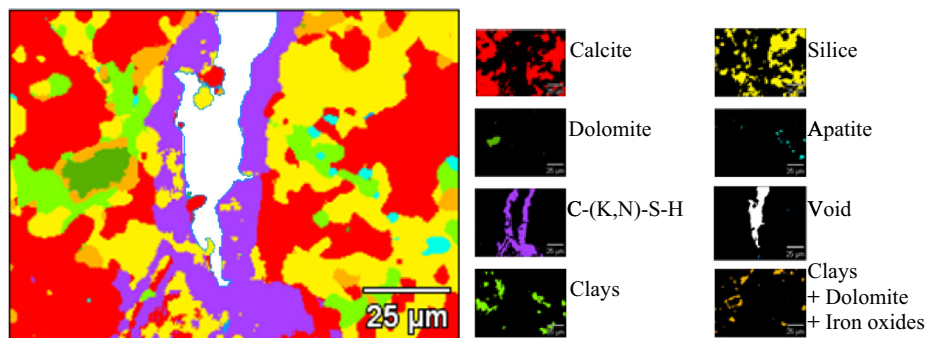

Fig. 14. Elemental X-ray images of the main phases present in Fig. 12B.

cracks may have the same orientations as the clay veins (Fig. 7B). In these cracks, ASR products are observed (Fig. 8A, C and D) by SEM-EDS analysis, with variable C/S ratios from 0.4 to 1.5 (Fig. 8E and F). Aggregates exhibit many microcracks around the micro-quartz (Fig. 9A and B). This micro-quartz of <10 μm is altered and presents alkalis from the SEM-EDS analyses with sodium in varying proportions (Fig. 9C). In contrast, larger quartz particles >20 μm do not appear altered (Fig. 9B), and SEM-EDS analyses do not detect alkalis (Fig. 9D). The clinker substitution by 30 wt% burnt oil shale (cT+fT+BOS2), reduces micro cracks and macrocracks (Fig. 10). Rarely, macrocracks (Fig. 11A) contain gel reaction products at a 0.3 C/S ratio (Fig. 11B). The micro-quartz seems only slightly altered (Fig. 10A and B) and shows no alkali or low proportion by SEM-EDS analyses (Fig. 10C and D). The quartz particles larger than 20 μm are not impaired (Fig. 10B), and alkalis are not detected through SEM-EDS analyses (Fig. 10D).

4.2.2.2. "cS+fS". The present study shows that concrete incorporating siliceous limestone S without mineral addition (cS+fS+BOS0) exhibits an altered aggregate morphology under SEM. In concrete cS+fS+BOS0, limestone aggregates are characterised by large cracks such as in concrete based on siliceous limestone T (Fig. 12A) with ASR products (Fig. 12B). An elemental X-ray image

points out the presence of alkalis (sodium and potassium) (Fig. 13). The reaction products, rich in alkalis, are said to be C—(K,N)—S—H identified by the treatment with the Compass software with a C/S ratio of approximately 0.5 (Fig. 14). SEM observations are also evidenced by micro-cracks between the micro- to crypto-quartz (<10 μm) and the limestone matrix (Fig. 15A and B). The silica in the form of coalescence of micro-quartz particles has cracks (Fig. 15C) as well as some alkalis (Fig. 15E). The larger quartz particles >20 μm were also observed and analysed (Fig. 15D) without alkalis (Fig. 15F). The addition of burnt oil shale at 30 wt% (cS+fS+BOS2) significantly reduces aggregate degradation related to ASR. Indeed, macrocracks are rarely observed and micro-cracks are reduced (Fig. 16A). In the cracks, reaction products are observed as gels (Fig. 17A) with a C/S ratio of approximately 0.3 (Fig. 17B). The silica does not exhibit marked deterioration. The micro-quartz does not present alkalis according to the EDS analysis (Fig. 16B). Similarly, quartz over 10 μm does not exhibit alkalis (Fig. 16C).

5. Discussion

In concrete incorporating flint and siliceous limestone aggregates, the microcrystalline quartz and the finely dispersed
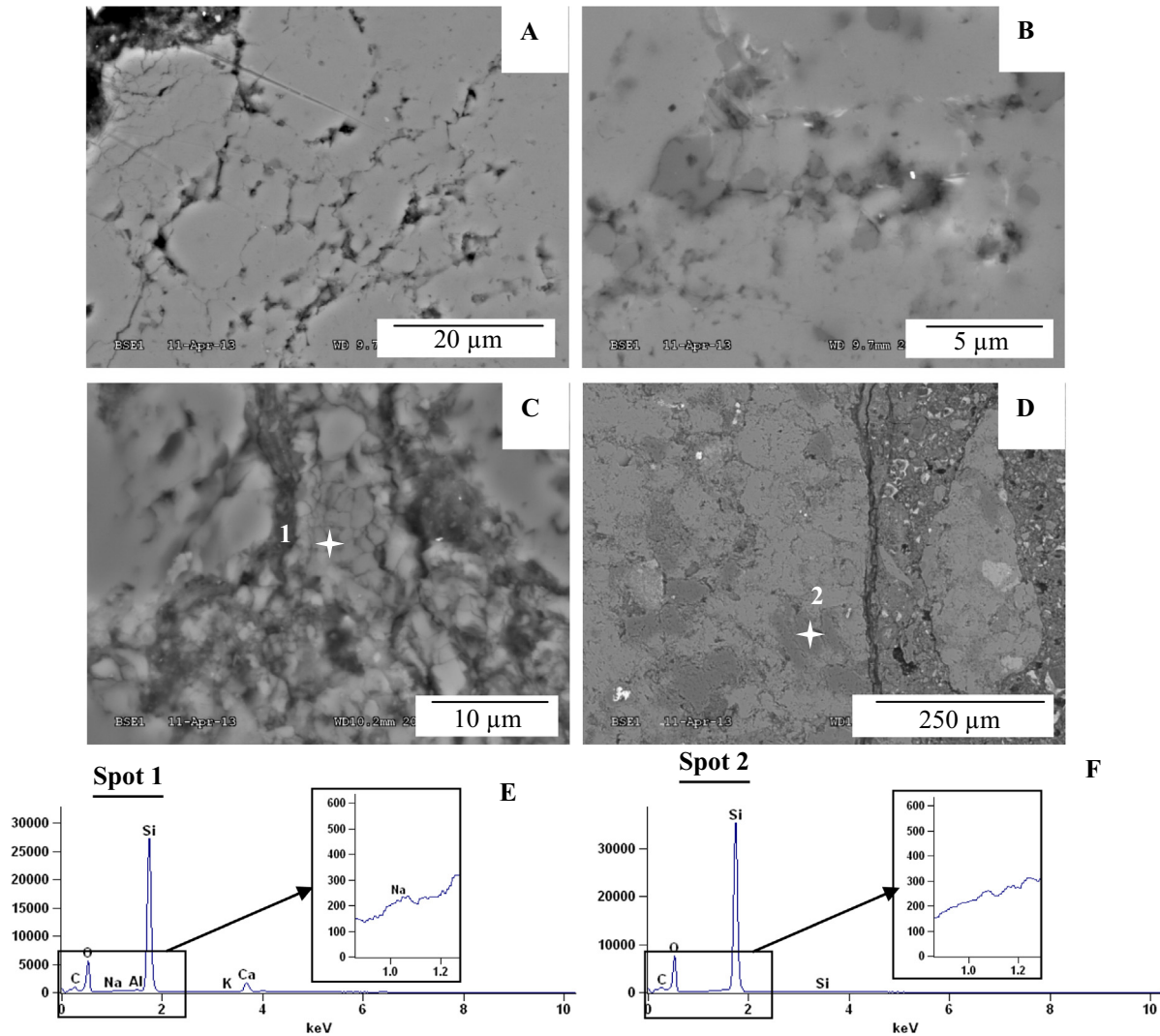
Fig. 15. Degraded siliceous limestone in concrete mixture cS+fS+BOS0: degraded micro-quartz (A), porous area around crypto-quartz (B), altered quartz particles coalescence (C) and undegraded quartz >20 μm (D). EDS spectrum of micro-quartz with alkalis Na from C (E) and large quartz without alkalis from D (F).

micro-quartz respectively neutralise alkalis until a threshold is reached. Without SCM – that is, BOS in this study – added in concrete, the neutralising capacity is exceeded generating a degradation of the aggregate and a longitudinal expansion of the concrete. From SEM observations, concrete mixtures without BOS have different degradation characteristics related to the ASR with impaired micromorphology aggregate as observed by Çopuroğlu et al. [4]. Indeed, the aggregates exhibit degraded facies with cracks, preferably in veins areas [70] as in aggregate T, and reaction products such as C—S—H gels rich in alkalis, resulting in the expansion of any concrete. The gel reaction products have a low C/S that can be explain by the high initial concentration of alkalis added to concrete, with sodium hydroxide influencing the gel composition [71–74]. The significant presence of alkalis in the siliceous phases evidences degradation. The degradation in concrete cC+fN+BOS0 is observed by an alteration in the microcrystalline quartz. In the case of the concrete mixtures based on siliceous limestone (cT+fT+BOS0 and cS+fS+BOS0), degradation of silica aggregates is observed by the presence of cracks around a micro-quartz of less than 10 μm and the alteration of this reactive form. Thus, the micro-quartz in siliceous limestone seems to be involved in the ASR as demonstrated by Guédon-Dubied et al. [58]. The reactivity of the latter

would be related to its size [75–79]. The microcrystalline quartz and the micro-quartz present alkalis when they are altered. Detected alkalis are sodium and potassium. The presence of alkalis in the reactive silica is consistent with the measured longitudinal expansions: the neutralization capacity of alkalis would be exceeded creating a degradation of silica in the aggregate and generating expansion.

To mitigate ASR, burnt oil shale was added to concrete. The substitution of clinker with burnt oil shale seemed to be beneficial for decreasing the alteration of siliceous aggregates and allows saving healthy zones with little or no alkalis without impairing mechanical performance as shown by numerous studies [24,25,27,37,80–84]. The use of burnt oil shale results in reducing the deterioration of microcrystalline silica in flint aggregate and the micro-quartz in siliceous limestones and the production of gel with a lower C/S [85–88] that can be mixed with ettringite [89] because of the presence of sulphates in the BOS. Indeed, sulphates have a high capacity of adsorption on C—S—H favoured by high temperature and basicity [90]. Regarding the flint aggregate, a pessimum effect was observed in previous studies [10,12,55]. This pessimum effect seems to be operated by adding only 17 wt% BOS (cC+fN+BOS1). Indeed, the addition of BOS that contains silica would play a
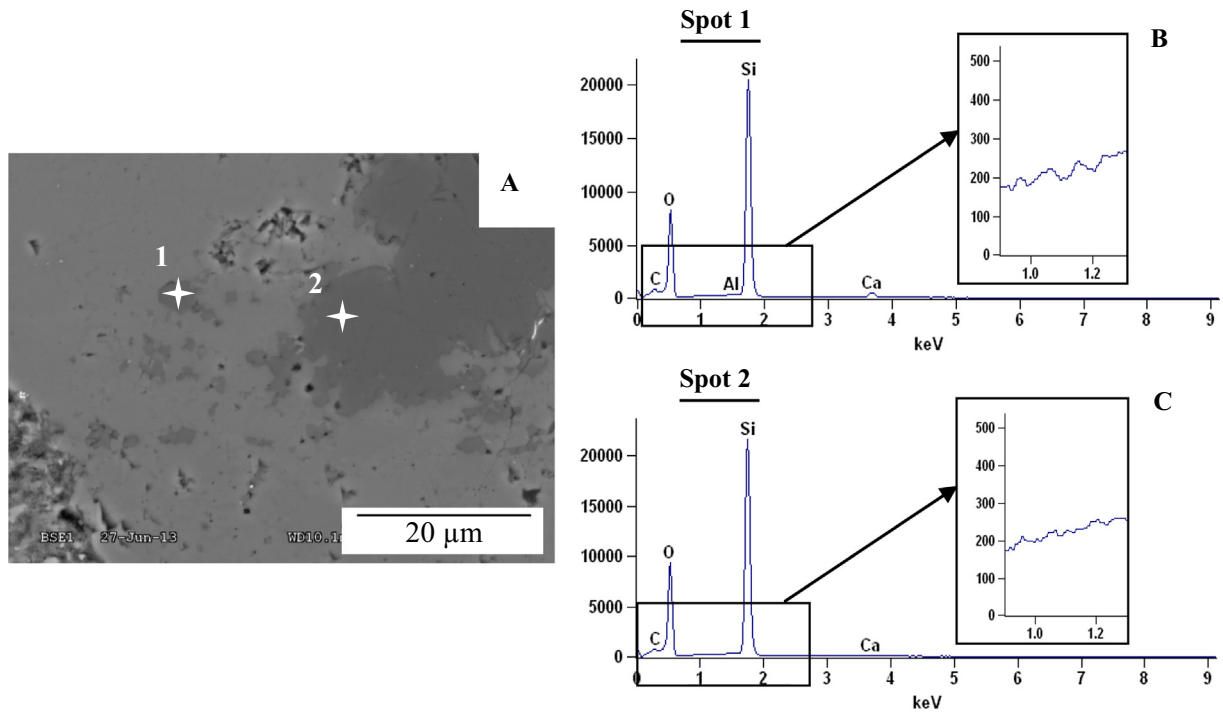
Fig. 16. Undegraded siliceous limestone in concrete mixture CS+FS+BOS2: undegraded micro-quartz and quartz >20 μm. EDS spectrum of micro-quartz without alkalis (B) and large quartz without alkalis (C).
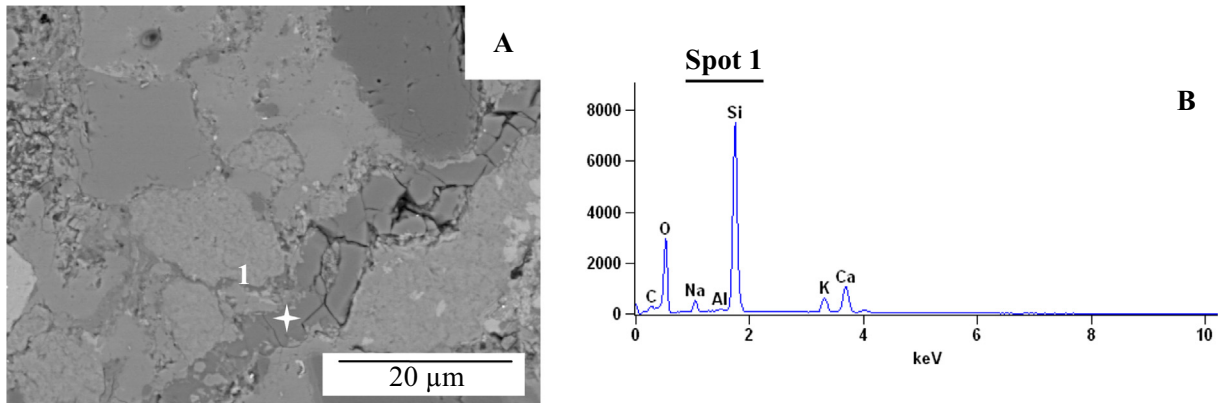

Fig. 17. Rare gels in siliceous limestone observed in concrete cS+fS+BOS2 (A). EDS spectrum of the C—S—H (B).

significant role. The silica in BOS could fix enough alkalis to avoid ASR development by not allowing the exceedance of the alkali neutralising capacity of the flint aggregate. In siliceous limestones aggregates, the micro-quartz aggregates of less than 10 μm are no longer degraded and only rarely have alkalis by adding 30 wt % BOS (cT+fT+BOS2 and cS+fS+BOS2). Thus, the pozzolanic reaction must set enough alkalis, to avoid the development of ASR products highlighted in concrete without burnt oil shale. The presence of reactive silica in oil shale would initiate the pozzolanic reaction [91]. In addition to the pozzolanic reaction generated by the burnt oil shale, the micro-quartz highlighted by Thiéry et al. [52] from an STEM study is probably more accessible and could neutralise alkalis, thereby decreasing the pore proportion of the alkalis in the micro-quartz aggregates. The microscopic observation can be correlated with macroscopic results. According to the calculation from Yeğinobali et al. [27], the addition of 17 wt% BOS reduces expansion from 87%, 53% and 45% for concretes based on flint aggregate and the two siliceous limestones T and S respectively. By adding

30 wt% BOS, the reduction is approximately 91% to 93%. Consequently, the addition of BOS allows for reducing the expansion due to ASR, similar as in other studies with reactive aggregates (chert or Pyrex glass) [27,42], by non-expansive pozzolanic C—S—H formation. Finally, BOS likewise has a positive impact on the mechanical properties by a small enhancement, with an optimum at 17 wt% BOS, that could be explained by the reduction of the cracks developed because of ASR and an increased amount of C—S—H [92,93].

6. Conclusion

The use of burnt oil shale (BOS) in concrete with reactive flint aggregate showed an immediate impact: concretes were low to only 0.01%, from the addition of 17 wt% of burnt oil shale (BOS1). The addition of BOS allows the operation of the pessimum effect of these concretes. For concrete mixes with siliceous limestone

aggregate, the action of BOS is more progressive and appears to be dependent on the substitution rate. Expansions decrease with the BOS addition rate and go to approximately 0.01% for a 30 wt% addition. The substitution of 30 wt% and 17 wt% of clinker by burnt oil shale results in a reduction in the degradation of the micro-quartz in siliceous limestones and microcrystalline silica in flint aggregate. Burnt oil shale would fix alkalis through non-expansive products generated by the pozzolanic reaction that would be initiated by the micro-quartz they contain. Thus, the action of burnt oil shale does not allow exceedance of the neutralisation capacity of alkalis in siliceous aggregate phases. Therefore, the results show a beneficial effect of burnt oil shale toward ASR in the presence of reactive aggregates with a reduction of the alteration of siliceous phases observed in petrography and consequently a concrete expansion reduction at 38 °C.

Acknowledgment

References

[1] D. Bulteel, E. Garcia-Diaz, C. Vernet, H. Zanni, Alkali–silica reaction: a method to quantify the reaction degree, Cem. Concr. Res. 32 (2002) 1199–1206, http://dx.doi.org/10.1016/S0008-8846(02)00759-7.

[2] D. Bulteel, N. Rafaï, P. Degrugilliers, E. Garcia-Diaz, Petrography study on altered flint aggregate by alkali-silica reaction, Mater. Charact. 53 (2004) 141–154, http://dx.doi.org/10.1016/j.matchar.2004.08.004.

[3] A.N.A. Mladenovič, S. Šturm, B. Mirtič, J.S. Šuput, Alkali silica reaction in mortars made from aggregates having different degrees of crystallinity, Ceram. Silikaty 53 (2009) 31–41.

[4] O. Çopuroğlu, Effect of silica dissolution on the mechanical characteristics of alkali-reactive aggregates, J. Adv. Concr. Technol. 8 (2010) 5–14, http://dx.doi.org/10.3151/jact.8.5.

[5] B. Fournier, R. Chevrier, M. De Grosbois, R. Lisella, K.J. Folliard, J.H. Ideker, et al., The accelerated concrete prism test (60 °C): variability of the test method and proposed expansion limits, in: 12th ICAAR, Beijing, China, 2004, pp. 314–323.

[6] Y. Monnin, P. Dégrugilliers, D. Bulteel, E. Garcia-Diaz, Petrography study of two siliceous limestones submitted to alkali-silica reaction, Cem. Concr. Res. 36 (2006) 1460–1466, http://dx.doi.org/10.1016/j.cemconres.2006.03.025.

[7] E. Garcia-Diaz, D. Bulteel, Y. Monnin, P. Degrugilliers, P. Fasseu, ASR pessimum behaviour of siliceous limestone aggregates, Cem. Concr. Res. 40 (2010) 546–549, http://dx.doi.org/10.1016/j.cemconres.2009.08.011.

[8] S. Multon, M. Cyr, A. Sellier, P. Diederich, L. Petit, Effects of aggregate size and alkali content on ASR expansion, Cem. Concr. Res. 40 (2010) 508–516, http://dx.doi.org/10.1016/j.cemconres.2009.08.002.

[9] Y. Monnin, P. Degrugilliers, D. Bulteel, E. Garcia-Diaz, Alkali-silica reaction on siliceous limestone: a method to measure the reaction degree, in: 12th ICAAR, Beijing, China, 2004, pp. 948–955.

[10] I. Moundoungou, D. Bulteel, E. Garcia-Diaz, P. Degrugilliers, The use of pessimum effect to reduce the expansion of concretes based on ASR reactive aggregates, in: 10th Int. Conf. Recent Advances Concr. Technol. Sustain. Issues, Seville, Spain, 2009. p. SP 261-16.

[11] F. Saint-Pierre, P. Rivard, G. Ballivy, Measurement of alkali-silica reaction progression by ultrasonic waves attenuation, Cem. Concr. Res. 37 (2007) 948–956, http://dx.doi.org/10.1016/j.cemconres.2007.02.022.

[12] I. Moundoungou, D. Bulteel, E. Garcia-Diaz, V. Thiéry, P. Dégrugilliers, J.G. Hammerschlag, Reduction of ASR expansion in concretes based on reactive chert aggregates: effect of alkali neutralisation capacity, Constr. Build. Mater. 54 (2014) 147–162, http://dx.doi.org/10.1016/j.conbuildmat.2013.12.036.

[13] J. Zelić, D. Rušić, D. Veža, R. Krstulović, Role of silica fume in the kinetics and mechanisms during the early stage of cement hydration, Cem. Concr. Res. 30 (2000) 1655–1662, http://dx.doi.org/10.1016/S0008-8846(00)00374-4.

[14] B.W. Langan, K. Weng, M.a. Ward, Effect of silica fume and fly ash on heat of hydration of Portland cement, Cem. Concr. Res. 32 (2002) 1045–1051, http://dx.doi.org/10.1016/S0008-8846(02)00742-1.

[15] B. Lothenbach, K. Scrivener, R.D. Hooton, Supplementary cementitious materials, Cem. Concr. Res. 41 (2011) 1244–1256, http://dx.doi.org/10.1016/j.cemconres.2010.12.001.

[16] G.J.Z. Xu, D.F. Watt, P.P. Hudec, Effectiveness of mineral admixtures in reducing ASR expansion, Cem. Concr. Res. 25 (1995) 1225–1236, http://dx.doi.org/10.1016/0008-8846(95)00115-S.

[17] N.Y. Mostafa, Q. Mohsen, S.A.S. El-Hemaly, S.A. El-Korashy, P.W. Brown, High replacements of reactive pozzolan in blended cements: microstructure and mechanical properties, Cem. Concr. Compos. 32 (2010) 386–391, http://dx.doi.org/10.1016/j.cemconcomp.2010.02.003.

[18] S.M.H. Shafaatian, A. Akhavan, H. Maraghechi, F. Rajabipour, How does fly ash mitigate alkali-silica reaction (ASR) in accelerated mortar bar test (ASTM C1567)?, Cem Concr. Compos. 37 (2013) 143–153, http://dx.doi.org/10.1016/j.cemconcomp.2012.11.004.

[19] M.C.G. Juenger, C.P. Ostertag, Alkali-silica reactivity of large silica fume-derived particles, Cem. Concr. Res. 34 (2004) 1389–1402, http://dx.doi.org/10.1016/j.cemconres.2004.01.001.

[20] B. Meng, P. Schiessl, The reaction of silica fume at early ages, in: 10th Int. Congr. Chem. Cem. vol. 3, Goteborg, 1997, p. 105.

[21] T.T.H. Bach, E. Chabas, I. Pochard, C. Cau Dit Coumes, J. Haas, F. Frizon, et al., Retention of alkali ions by hydrated low-pH cements: mechanism and Na+/K+ selectivity, Cem. Concr. Res. 51 (2013) 14–21, http://dx.doi.org/10.1016/j.cemconres.2013.04.010.

[22] A. Goldman, A. Bentur, The influence of microfillers on enhancement of concrete strength, Cem. Concr. Res. 23 (1993) 962–972.

[23] T. Khedaywi, A. Yeĝinobali, M. Smadi, J. Cabrera, Pozzolanic activity of Jordanian oil shale, Cem. Concr. Res. 20 (1990) 843–852, http://dx.doi.org/10.1016/0008-8846(90)90045-Y.

[24] A. Bentur, Application of oil shale ash as a building material, Silic. Indus. 7 (1982) 163–168.

[25] M.M. Smadi, R.H. Haddad, The use of oil shale ash in Portland cement concrete, Cem. Concr. Compos. 25 (2003) 43–50, http://dx.doi.org/10.1016/S0958-9465(01)00054-3.

[26] M. Winter, Spent oil shale use in earthwork construction, Eng. Geol. 60 (2001) 285–294, http://dx.doi.org/10.1016/S0013-7952(00)00109-5.

[27] A. Yeĝinobali, M. Smadi, T. Khedaywi, Effectiveness of oil shale ash in reducing alkali-silica reaction expansions, Mater. Struct. 26 (1993) 159–166, http://dx.doi.org/10.1007/BF02472933.

[28] L. Malvar, G. Cline, D. Burke, R. Rollings, T. Sherman, J. Greene, Alkali-silica reaction mitigation: state-of-the art and recommendations, Am. Concr. Inst. Mater. J. 99 (2002) 1–14.

[29] S. Diamond, Alkali silica reactions—some paradoxes, Cem. Concr. Compos. 19 (1997) 391–401, http://dx.doi.org/10.1016/S0958-9465(97)00004-8.

[30] VNU Science Press, Solid fuel mineral deposits, in: Proc. 27th Int. Geol. Congree, Moscow, 1984.

[31] European Academies Science Advisory Council, A study on the EU oil shale industry – viewed in the light of the Estonian experience, 2007.

[32] J.R. Dyni, Geology and resources of some world oil-shale deposits: U.S. Geological Survey Scientific Investigations Report, 2006.

[33] World Energy Council, 2010 Survey of energy resources, London, 2010.

[34] A. Thevarasah, M. Selvaratnam, Some studies on pozzolanic cement, J. Natl. Sci. Found. Sri Lanka 7 (1979) 57–63.

[35] A. Cheng, S.J. Chao, W.T. Lin, Effect of calcination temperature on pozzolanic reaction of calcined shale mortar, Appl. Mech. Mater. 174–177 (2012) 843–846. doi:10.4028/www.scientific.net/AMM.174-177.843.

[36] X. Feng, X. Niu, X. Bai, X. Liu, H. Sun, Cementing properties of oil shale ash, J. China Univ. Min. Technol. 17 (2007) 498–502, http://dx.doi.org/10.1016/S1006-1266(07)60133-3.

[37] M.M. Smadi, A. Yeĝinobali, T. Khedaywi, Potential uses of Jordanian spent oil shale ash as a cementine material 41 (1989) 183–190.

[38] C. Shi, R.L. Day, Comparison of different methods for enhancing reactivity of pozzolans, Cem. Concr. Res. 31 (2001) 813–818, http://dx.doi.org/10.1016/S0008-8846(01)00481-1.

[39] C. Shi, An overview on the activation of reactivity of natural pozzolans, Can. J. Civ. Eng. 28 (2001) 778–786, http://dx.doi.org/10.1139/l01-041.

[40] G. Habert, N. Choupay, J.M. Montel, D. Guillaume, G. Escadeillas, Effects of the secondary minerals of the natural pozzolans on their pozzolanic activity, Cem. Concr. Res. 38 (2008) 963–975, http://dx.doi.org/10.1016/j.cemconres.2008.02.005.

[41] E. Vejmelková, M. Keppert, P. Rovnaníková, Z. Keršner, R. Černý, Application of burnt clay shale as pozzolan addition to lime mortar, Cem. Concr. Compos. 34 (2012) 486–492, http://dx.doi.org/10.1016/j.cemconcomp.2012.01.001.

[42] T.E. Stanton, Studies of use of pozzolans for counteracting excessive concrete expansion resulting from reaction between aggregates and the alkalies in cement, in: Symp. Use Pozzolanic Mater. Mortars Concr., ASTM STP-99, Philadelphia, 1950, pp. 178–203.

[43] C. Knutson, R. Smith, B. Russell, History and some potentials of on shale cement, in: 22nd Oil Shale Symp. Proc. Color. Sch. Mines, Golden, Colorado, 1989, pp. 184–198.

[44] V.R. Rohrbach, Herstellung von Ölschieferzement und Gewinnung elektrischer Energie aus Ölschiefer nach dem Rohrbach-Lurgi-Verfahren, Zement-Kalk-Gips Int. 7 (1969) 293–296.

[45] V.F. Feige, Zur wirtschaftlichen Verwertung des Ölschiefers bei Rohrbach, Zement-Kalk-Gips Int. 2 (1992) 54–62.

[46] A. Frimmel, W. Oschmann, L. Schwark, Chemostratigraphy of the Posidonia Black Shale, SW Germany I. Influence of sea-level variation on organic facies evolution, Chem. Geol. 206 (2004) 199–230, http://dx.doi.org/10.1016/j.chemgeo.2003.12.007.

[47] A.Y. Al-Otoom, Utilization of oil shale in the production of Portland clinker, Cem. Concr. Compos. 28 (2006) 3–11, http://dx.doi.org/10.1016/j.cemconcomp.2005.06.006.

[48] H. Wefing, Oil shale is integral part of German cement process, Rock Prod. Cem. (1981).

[49] V.J. Wuhrer, Hydraulische Bindemittel aus Ölschiefer, Zement-Kalk-Gips Int. 3 (1950).

[50] M. Riedhammer, The Rohrbach process – the economical alternative method of utilizing oil shale, TIZ-Fachberichte 109 (1985) 941–944.

[51] J. Hilger, Combined utilization of oil shale energy and oil shale minerals within the production of cement and other hydraulic binders, Oil Shale 20 (2003) 347–355. http://www.kirj.ee/public/oilshale/8_hilger_2003_3s.pdf.

[52] V. Thiéry, A. Bourdot, D. Bulteel, Characterization of raw and burnt oil shale from Dotternhausen: petrographical and mineralogical evolution with temperature, Mater. Charact. 106 (2015) 442–451, http://dx.doi.org/10.1016/j.matchar.2015.06.022.

[53] V. Matterne, S. Lepetz, Élevage et agriculture dans le Nord de la Gaule durant l'époque gallo-romaine: une confrontation des données archéologiques et carpologiques, Rev. Archéologique Picardie (2003) 23–35. http://www.persee.fr/web/revues/home/prescript/article/pica_0752-5656_2003_num_1_1_2354.

[54] Y. Monnin, Methodologie pour décrire le gonflement multi-échelle de calcaires siliceux soumis à la réaction alcali-silice dans le matériau béton, Ecole des Mines de Douai et Université d'Artois, 2005.

[55] I. Moundoungou, Une étude de faisabilité pour une meilleure utilisation dans le matériau béton de granulats «potentiellement réactifs» vis-à-vis de la réaction alcali-silice, Ecole des Mines de Douai et Université de Lille 1, 2010.

[56] R.I. Murchison, On the geological structure of the Alps, Apennines and Carpathians, more especially to prove a transition from secondary to tertiary rocks, and the development of Eocene deposits in Southern Europe. Part II, Q. J. Geol. Soc. 5 (1849). 328–328.

[57] O.W. Flörke, H. Graetsch, B. Martin, K. Röller, R. Wirth, Nomenclature of micro- and non-crystalline silica minerals, based on structure and microstructure, Neues Jahrb. Mineral. Abh. 163 (1991) 19–42.

[58] J.S. Guédon-Dubied, G. Cadoret, V. Durieux, F. Martineau, F. Fasseu, V. Overkeke, Etude du calcaire Tournaisien de la carriere Cimescaut à Antoing (Belgique). Analyse pétrographique et chimique et réactivité aux alcalins, Bull. Des Lab. Des Ponts Chaussées 226 (2000) 57–66.

[59] I. Sims, P. Nixon, RILEM recommended test method AAR-I: detection of potential alkali-reactivity of aggregates-Petrographic method, Mater. Struct. 36 (2003) 480–496, http://dx.doi.org/10.1617/14060.

[60] P.E. Grattan-Bellew, L.D. Mitchell, J. Margeson, D. Min, Is alkali-carbonate reaction just a variant of alkali-silica reaction ACR = ASR?, Cem Concr. Res. 40 (2010) 556–562, http://dx.doi.org/10.1016/j.cemconres.2009.09.002.

[61] AFNOR NF EN 196-1, Methods of testing cement – Part 1: Determination of strength, 2006.

[62] AFNOR NF EN 450-1, Fly ash for concrete. Part 1: Definition, specifications and conformity criteria, 2005.

[63] British standard BS 3892, Pulverised fuel-ash. Part 1: specification for pulverized fuel ash for use with Portland cement, 1997.

[64] ASTM C618, Standard specification for coal fly ash and raw or calcined natural pozzolan for use in concrete, 2003.

[65] AFNOR NF P18-454, Béton, Réactivité d'une formule de béton vis-à-vis de l'alcali-réaction, essai de performance, 2004.

[66] AFNOR FD P18-456, Béton, Réactivité d'une formule de béton vis-à-vis de l'alcali-réaction, critères d'interprétation des résultats de l'essai de performance, 2004.

[67] R. Castaing, Application des sondes électroniques à une méthode d'analyse ponctuelle chimique et cristallographique, Université de Paris, 1951.

[68] M. Beyene, A. Snyder, R.J. Lee, M. Blaszkiewicz, Alkali Silica Reaction (ASR) as a root cause of distress in a concrete made from Alkali Carbonate Reaction (ACR) potentially susceptible aggregates, Cem. Concr. Res. 51 (2013) 85–95, http://dx.doi.org/10.1016/j.cemconres.2013.04.014.

[69] P. Virmani, F. Faridazar, Alkali-Silica Reaction Mechanisms and Detection: An Advanced Understanding, TECHBRIEF, 2014.

[70] H.W. Reinhardt, O. Mielich, A fracture mechanics approach to the crack formation in alkali-sensitive grains, Cem. Concr. Res. 41 (2011) 255–262, http://dx.doi.org/10.1016/j.cemconres.2010.11.008.

[71] E.B. Nelson, G.L. Kalousek, Effects of Na₂O on calcium silicate hydrates at elevated temperatures, Cem. Concr. Res. 7 (1977) 687–694, http://dx.doi.org/10.1016/0008-8846(77)90052-7.

[72] S.-Y. Hong, F.P. Glasser, Alkali binding in cement pastes. Part I. The C–S–H phase, Cem. Concr. Res. 29 (1999) 1893–1903, http://dx.doi.org/10.1016/S0008-8846(99)00187-8.

[73] W. Nocun-Wczelik, Effect of Na and Al on the phase composition and morphology of autoclaved calcium silicate hydrates, Cem. Concr. Res. 29 (1999) 1759–1767, http://dx.doi.org/10.1016/S0008-8846(99)00166-0.

[74] I. García Lodeiro, D.E. Macphee, A. Palomo, A. Fernández-Jiménez, Effect of alkalis on fresh C–S–H gels. FTIR analysis, Cem. Concr. Res. 39 (2009) 147–153. 10.1016/j.cemconres.2009.01.003.

[75] Š. Lukschová, R. Přikryl, Z. Pertold, Petrographic identification of alkali-silica reactive aggregates in concrete from 20th century bridges, Constr. Build. Mater. 23 (2009) 734–741, http://dx.doi.org/10.1016/j.conbuildmat.2008.02.020.

[76] P. Alaejos, V. Lanza, Influence of equivalent reactive quartz content on expansion due to alkali silica reaction, Cem. Concr. Res. 42 (2012) 99–104, http://dx.doi.org/10.1016/j.cemconres.2011.08.006.

[77] P.M. Dove, Kinetic and thermodynamic controls on silica reactivity in weathering environments. Chemical weathering rates of silicate minerals, in: A. White, S. Brantley (Eds.), Rev. Mineral., Mineralogical Society of America, Washington (DC), 1995, pp. 235–290.

[78] B.J. Wigum, Examination of microstructural features of Norwegian cataclastic rocks and their use of predicting alkali-reactivity in concrete, Eng. Geol. 40 (1995) 195–214.

[79] B.J. Wigum, M. Haugen, O. Skjølsvold, J. Lindgård, Norwegian petrographic method – development and experiences during a decade of service, in: 12th ICAAR, 2004.

[80] H. Baum, A. Bentur, I. Soroka, Properties and structure of oil shale ash pastes. II: Mechanical properties and structure, Cem. Concr. Res. 15 (1985) 391–400, http://dx.doi.org/10.1016/0008-8846(85)90112-7.

[81] N.Q. Feng, S.Y.N. Chan, Z.S. He, M.K.C. Tsang, Shale ash concrete, Cem. Concr. Compos. 27 (1997) 279–291.

[82] J. Valek, J.J. Hughes, C.J.W.P. Groot, Historic mortars with burned alum shale as an artificial pozzolan, in: Springer Science & Business Media (Ed.), Hist. Mortars Characterisation, Assess. Repair, 2012, pp. 7–88. https://books.google.fr/books?id=O7gTczZdXwAC.

[83] M. Ish-Shalom, A. Bentur, T. Grinberg, Cementing properties of oil shales ash – 1. Effect of burning method and temperature, Cem. Concr. Res. 10 (1980) 799–807, http://dx.doi.org/10.1016/0008-8846(80)90008-3.

[84] W. Kikas, K. Ojaste, L. Raado, Ursache und Wirkungsweise der Alkalireaktion in den aus estnischem Portlandölschieferzement hergestellten Betonen, Zement-Kalk-Gips Int. 52 (1999) 106–111.

[85] M.S.Y. Bhatty, N.R. Greening, Interaction of alkalis with hydrating and hydrated calcium silicates, in: Proc. 4th Int. Conf. Eff. Alkalis Cem. Concr., Purdue, 1978, pp. 87–112.

[86] J. Duchesne, M.A. Bérubé, Effect of supplementary cementing materials on the composition of cement hydration products, Adv. Cem. Based Mater. 2 (1995) 43–52, http://dx.doi.org/10.1016/1065-7355(95)90024-1.

[87] W. Aquino, D.a. Lange, J. Olek, The influence of metakaolin and silica fume on the chemistry of alkali – silica reaction products, Cem. Concr. Compos. 23 (2001) 485–493.

[88] H. El-Didamony, M. Heikal, S. Abd El Aleem, Influence of delayed addition time of sodium sulfanilate phenol formaldehyde condensate on the hydration characteristics of sulfate resisting cement pastes containing silica fume, Constr. Build. Mater. 37 (2012) 269–276, http://dx.doi.org/10.1016/j.conbuildmat.2012.07.023.

[89] M. Uibu, P. Somelar, L.-M. Raado, N. Irha, T. Hain, A. Koroljova, et al., Oil shale ash based backfilling concrete – strength development, mineral transformations and leachability, Constr. Build. Mater. 102 (2016) 620–630, http://dx.doi.org/10.1016/j.conbuildmat.2015.10.197.

[90] L. Divet, R. Randriambololona, Delayed ettringite formation: the effect of temperature and basicity on the interaction of sulphate and C–S–H phase, Cem. Concr. Res. 28 (1998) 357–363, http://dx.doi.org/10.1016/S0008-8846(98)00006-4.

[91] A. Bentur, M. Ish-Shalom, M. Ben-Bassat, T. Grinberg, Properties and application of oil shale ash, Am. Concr. Inst. (1986) 779–802.

[92] A. Oner, S. Akyuz, R. Yildiz, An experimental study on strength development of concrete containing fly ash and optimum usage of fly ash in concrete, Cem. Concr. Res. 35 (2005) 1165–1171, http://dx.doi.org/10.1016/j.cemconres.2004.09.031.

[93] V.G. Papadakis, S. Antiohos, S. Tsimas, Supplementary cementing materials in concrete. Part II: A fundamental estimation of the efficiency factor, Cem. Concr. Res. 32 (2002) 1533–1538, http://dx.doi.org/10.1016/S0008-8846(02)00829-3.